Hindawi Publishing Corporation
Mathematical Problems in Engineering
Volume 2015, Article ID 514612, 8 pages
http://dx.doi.org/10.1155/2015/514612

Research Article

Biobjective Optimization of Vibration Performance of Steel-Spring Floating Slab Tracks by Four-Pole Parameter Method Coupled with Ant Colony Optimization

Hao Jin,[1] Weining Liu,[2] Shunhua Zhou,[1] and Christoph Adam[3]

[1]*Key Laboratory of Road and Traffic Engineering of Ministry of Education, Tongji University, Shanghai 201804, China*
[2]*School of Civil Engineering, Beijing Jiaotong University, Beijing 100044, China*
[3]*Department of Civil Engineering Sciences, University of Innsbruck, Technikerstraße 13, 6020 Innsbruck, Austria*

Correspondence should be addressed to Hao Jin; zhujijinhao@gmail.com

Received 24 March 2015; Revised 10 July 2015; Accepted 13 July 2015

Academic Editor: Domenico Mundo

Steel-spring floating slab tracks are one of the most effective methods to reduce vibrations from underground railways, which has drawn more and more attention in scientific communities. In this paper, the steel-spring floating slab track located in *Track Vibration Abatement and Control Laboratory* was modeled with four-pole parameter method. The influences of the fastener damping ratio, the fastener stiffness, the steel-spring damping ratio, and the steel-spring stiffness were researched for the rail displacement and the foundation acceleration. Results show that the rail displacement and the foundation acceleration will decrease with the increase of the fastener stiffness or the steel-spring damping ratio. However, the rail displacement and the foundation acceleration have the opposite variation tendency for the fastener damping ratio and the steel-spring stiffness. In order to optimize the rail displacement and the foundation acceleration affected by the fastener damping ratio and the steel-spring stiffness at the same time, a multiobjective ant colony optimization (ACO) was employed. Eventually, Pareto optimal frontier of the rail displacement and the foundation acceleration was derived. Furthermore, the desirable values of the fastener damping ratio and the steel-spring stiffness can be obtained according to the corresponding Pareto optimal solution set.

1. Introduction

Vibrations generated by underground railways are one of the most serious engineering problems. Waves induced by the dynamic interaction between the train wheels and the rails propagate from the surrounding soils to the foundations of nearby buildings, resulting in structural vibrations and reradiated noise. One of the most effective methods to reduce vibrations from underground railways is to use floating slab tracks that rest on the steel-springs. In the last decades, steel-spring floating slab tracks are largely used, especially in China.

Therefore, many scientists apply themselves to improve vibration performance of steel-spring floating slab tracks. Zhai et al. [1–3] developed a coupled dynamic computation model for metro vehicles, along with a steel-spring floating slab track. Using the developed model, they analyzed the influences of the thickness, length, and mass of floating-slab, spring rate and its arrangement space, running speed, and so forth on the time and frequency domain characteristics of steel-spring fulcrum force. Ding et al. [4, 5] also analyzed the vibration parameters of the steel-spring floating slab track using MIDAS/GTS. Lei and Jiang [6] built the model of a steel-spring floating slab track using FEM. The density, the thickness, and the length of the floating slab as well as the isolator stiffness were researched based on modal analysis and the harmonic response analysis. Gu and Zhang [7] established a continuous 3D finite element model for steel-spring floating slab track using ANSYS. The dynamic transfer characteristics and the isolation effect of this kind of track structure were studied for different design parameters and actuation frequency. Beside theoretical analysis, some lab tests and in-site tests were performed. Liu et al. [8] carried out low-frequency vibration tests on the steel-spring floating slab

Figure 1: The steel-spring floating slab track in *Track Vibration Abatement and Control Laboratory*.

track in *Track Vibration Abatement and Control Laboratory* at Beijing Jiaotong University and studied the influence of the stiffness and spacing of steel-springs. Li et al. [9] tested vibration reduction ability of the steel-spring floating slab track of Beijing metro line 5 in China.

The present contribution aims to optimize vibration performance of steel-spring floating slab tracks with four-pole parameter method coupled with ACO. This paper is organized as follows. Section 2 describes how to model the steel-spring floating slab track with four-pole parameter method. Then, two optimization objectives are represented in Section 3. In Section 4, optimization variables are decided. A multiobjective ACO was introduced in Section 5. In Section 6, the floating slab track is optimized. Conclusions are in Section 7.

2. Mathematical Model

There is one unit of steel-spring floating slab tracks (see Figure 1) in *Track Vibration Abatement and Control Laboratory*, which is the only underground laboratory for track vibration research in Asia.

Figure 2 shows plan and cross section of the steel-spring floating slab track. The length l_{rail} of each rail is 6000 mm. The distance between the fasteners is 600 mm and the distance between the steel-springs is 1200 mm. The length of the floating slab l_b is 6000 mm, the width $d_b = 3500$ mm, and the height $h_b = 450$ mm.

The steel-spring floating slab track was simplified (see Figure 3). Then, four-pole parameter method, which is a simple and effective method to solve the dynamic system [10], was employed to model it.

According to Figure 3, the floating slab track system can be divided into four subsystems: the rail subsystem, the fastener subsystem, the floating slab subsystem, and the steel-spring subsystem. The relations of the subsystems are demonstrated in Figure 4.

Therefore, the four-pole parameter matrix of the rail subsystem including only one rail is

$$\mathbf{S}_{\text{rail}}^{1(2)} = \begin{bmatrix} 1 & j\omega m_{\text{rail}} \\ 0 & 1 \end{bmatrix}. \tag{1}$$

The four-pole parameter matrix of the fastener subsystem consisting of ten fasteners is

$$\mathbf{S}_f^{1(2)} = \begin{bmatrix} 1 & 0 \\ \dfrac{j\omega}{\left[10 \times k_f \left(1 + 2j\xi_f\right)\right]} & 1 \end{bmatrix}. \tag{2}$$

The four-pole parameter matrix of the floating slab subsystem is

$$\mathbf{S}_b = \begin{bmatrix} 1 & j\omega m_b \\ 0 & 1 \end{bmatrix}. \tag{3}$$

The four-pole parameter matrix of the steel-spring subsystem having five steel-springs is

$$\mathbf{S}_{\text{ss}}^{1(2)} = \begin{bmatrix} 1 & 0 \\ \dfrac{j\omega}{\left[5 \times k_{\text{ss}} \left(1 + 2j\xi_{\text{ss}}\right)\right]} & 1 \end{bmatrix}, \tag{4}$$

where j is the imaginary number, ω is the angular frequency, m_{rail} is the mass of one rail, and m_b is the mass of the floating slab. The stiffness of a direction fixation fastener is k_f N/m and the damping ratio is ξ_f. The stiffness of a steel-spring is k_{ss} N/m and the damping ratio is ξ_{ss}.

The floating slab track is assumed to be located on a concrete foundation which is a simply supported slab on four edges. The length of the foundation is b_c, the width is a_c, and the height is c_c. u and v are the equivalent position where the floating slab track forces. The distance between $u(v)$ and o is $b_1(b_2)$. Figure 5 gives the details about the foundation.

As a consequence, the mobility equation of the foundation is

$$\begin{Bmatrix} V_f^1 \\ V_f^2 \end{Bmatrix} = \mathbf{Y} \cdot \begin{Bmatrix} F_f^1 \\ F_f^2 \end{Bmatrix} = \begin{bmatrix} \mathbf{Y}_{11} & \mathbf{Y}_{12} \\ \mathbf{Y}_{21} & \mathbf{Y}_{22} \end{bmatrix} \cdot \begin{Bmatrix} F_f^1 \\ F_f^2 \end{Bmatrix}, \tag{5}$$

in which $F_f^{1(2)}(f)$ is the response force of the foundation at the position $u(v)$ and $V_f^{1(2)}(f)$ is the response velocity of the foundation at the position $u(v)$. $\mathbf{Y}$ is the mobility matrix, which is presented as follows [11]:

$$\begin{aligned}
\mathbf{Y}_{11} &= \left(\frac{j\omega}{m_c}\right) \cdot \sum_{m=1}^{\infty} \sum_{n=1}^{\infty} \left\{ \frac{\varphi_{mn}^2 \left(a_c/2 - b_1, b_c/2\right)}{\left[\omega_{mn}^2 \cdot \left(1 + j\eta_c\right) - \omega^2\right]} \right\}, \\
\mathbf{Y}_{12} &= \left(\frac{j\omega}{m_c}\right) \\
&\quad \cdot \sum_{m=1}^{\infty} \sum_{n=1}^{\infty} \left\{ \frac{\varphi_{mn} \left(a_c/2 - b_1, b_c/2\right) \varphi_{mn} \left(a_c/2 + b_2, b_c/2\right)}{\left[\omega_{mn}^2 \cdot \left(1 + j\eta_c\right) - \omega^2\right]} \right\}, \\
\mathbf{Y}_{21} &= \left(\frac{j\omega}{m_c}\right) \\
&\quad \cdot \sum_{m=1}^{\infty} \sum_{n=1}^{\infty} \left\{ \frac{\varphi_{mn} \left(a_c/2 + b_2, b_c/2\right) \varphi_{mn} \left(a_c/2 - b_1, b_c/2\right)}{\left[\omega_{mn}^2 \cdot \left(1 + j\eta_c\right) - \omega^2\right]} \right\}, \\
\mathbf{Y}_{22} &= \left(\frac{j\omega}{m_c}\right) \cdot \sum_{m=1}^{\infty} \sum_{n=1}^{\infty} \left\{ \frac{\varphi_{mn}^2 \left(a_c/2 + b_2, b_c/2\right)}{\left[\omega_{mn}^2 \cdot \left(1 + j\eta_c\right) - \omega^2\right]} \right\},
\end{aligned} \tag{6}$$

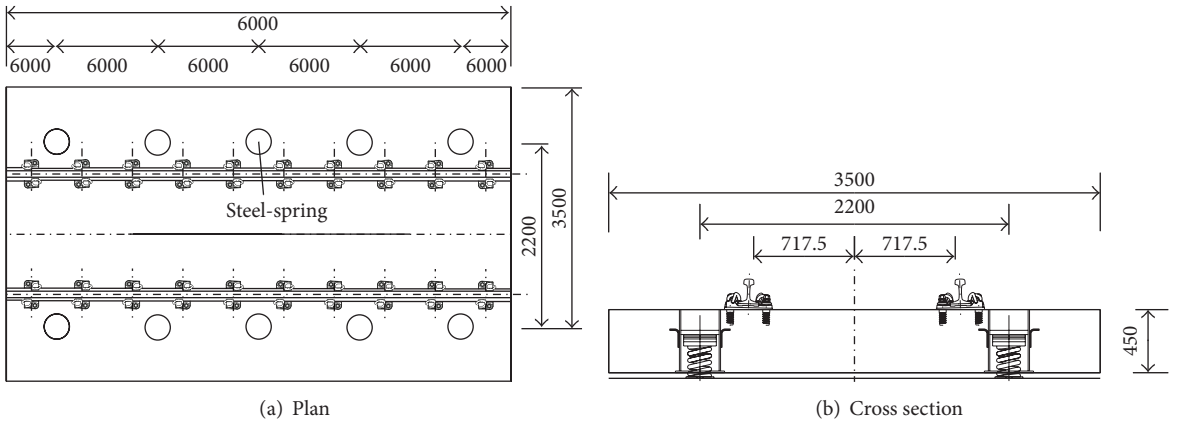

(a) Plan (b) Cross section

Figure 2: Plan and cross section of the steel-spring floating slab track (unit: mm).

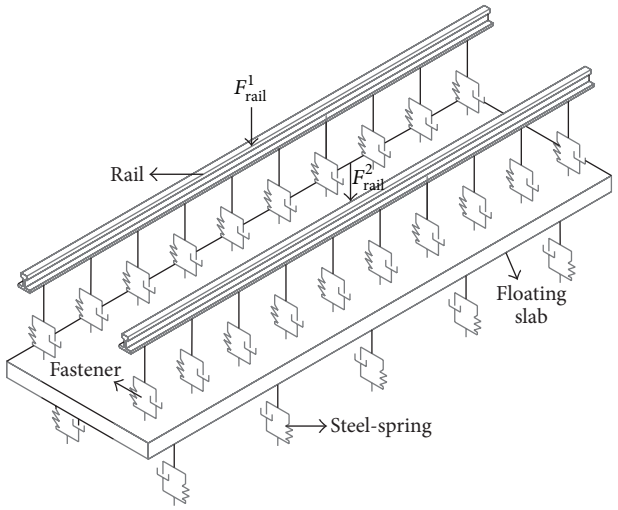

Figure 3: The simplified model of the steel-spring floating slab track.

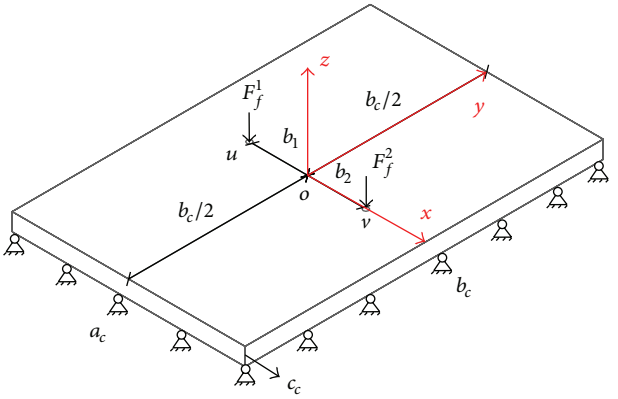

Figure 5: The sizes of the foundation.

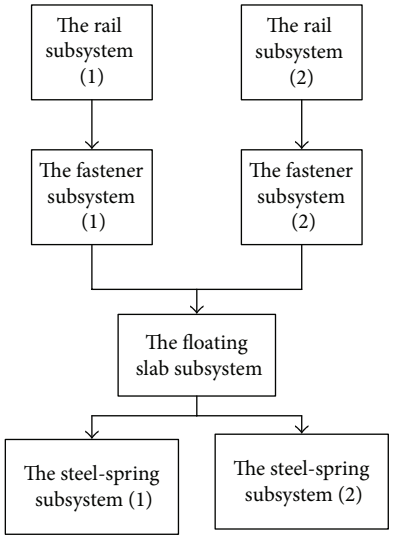

Figure 4: The relations of the subsystems.

where

(i) $\omega_{mn} = \pi^2(m^2/a_c^2 + n^2/b_c^2)[D/(\rho_c c_c)]^{1/2}$ is the resonance frequency of the foundation, the parameter $D = E_c c_c^3/[12(1-\upsilon_c^2)]^2$, m_c is the mass of the foundation, and the angular frequency $\omega = 2\pi f$;

(ii) $\varphi_{mn} = 2\sin(m\pi x/a_c)\sin(n\pi y/b_c)$ is the normalized mode shape, $m = 1, 2, \ldots, \infty$, $n = 1, 2, \ldots, \infty$;

(iii) the density of the foundation $\rho_c = 2680\,\text{kg/m}^3$, Young's modulus $E_c = 4 \times 10^{10}$ Pa, the Poisson ratio $\upsilon_c = 0.3$, and the material loss factor $\eta_c = 0.025$.

Suppose that $F_f^1 = F_f^2$, so we can get $V_f^1/F_f^1 = \mathbf{Y}_{11} + \mathbf{Y}_{12}$ and $V_f^2/F_f^2 = \mathbf{Y}_{21} + \mathbf{Y}_{22}$ from (5).

According to Figure 4, we can get the equation

$$\begin{Bmatrix} F_{\text{rail}}^{1(2)} \\ V_{\text{rail}}^{1(2)} \end{Bmatrix} = \mathbf{S} \begin{Bmatrix} F_f^{1(2)} \\ V_f^{1(2)} \end{Bmatrix} = \mathbf{S}_{\text{rail}}\mathbf{S}_f\mathbf{S}_b\mathbf{S}_{\text{ss}} \begin{Bmatrix} F_f^{1(2)} \\ V_f^{1(2)} \end{Bmatrix}, \quad (7)$$

where the exciting force, which is set in the middle of the rail (see Figure 3), $F_{\text{rail}}^{1(2)}(f)$ equals 1 at the frequency f.

By (1)~(5) and (7), the response force of the foundation at the position $u(v)$ can be written as

$$F_f^{1(2)}(f) = \left\{ \left[1 + j\omega m_{\text{rail}} \cdot \frac{j\omega}{\left(10k_f\left(1+2j\xi_f\right)\right)} \right] + \left[\frac{j\omega}{5\left(k_{\text{ss}}\left(1+2j\xi_{\text{ss}}\right)\right)} + M^{1(2)} \right] \cdot \left[j\omega m_b \left(1 + j\omega m_{\text{rail}} \cdot \frac{j\omega}{\left(10 \times k_f\left(1+2j\xi_f\right)\right)} \right) + j\omega m_{\text{rail}} \right] \right\}^{-1} F_{\text{rail}}^{1(2)}(f), \tag{8}$$

in which the parameters $M^1 = V_f^1/F_f^1$ and $M^2 = V_f^2/F_f^2$.

The response velocity of the foundation at the position $u(v)$ is represented as follows:

$$V_f^{1(2)}(f) = M^{1(2)} \cdot F_f^{1(2)}. \tag{9}$$

The response velocity of the rail is

$$V_{\text{rail}}^{1(2)}(f) = \mathbf{S}_{21} \cdot F_f^{1(2)} + \mathbf{S}_{22} \cdot V_f^{1(2)}. \tag{10}$$

3. Optimization Objectives

The vibrations induced by the interaction between the wheels and the rails are transferred from the rails to the foundation and then propagate to the foundations of the nearby buildings which will result in structure vibrations and reradiated noise. Therefore, the foundation vibration reflects the structure vibration. In order to reduce the structure vibration, the foundation vibration should be reduced firstly. Consequently, the foundation acceleration is set as the first optimization objective. The objective function is

$$\min a_f = 20 \times \log_{10}\left(\frac{a_f'}{a_0}\right). \tag{11}$$

The large vibration displacement of the rail usually makes unsafety and instability of the railway operation. Therefore, the vibration displacement of the rail is set as the second optimization objective. The objective function is given as follows:

$$\min d_{\text{rail}} = 20 \times \log_{10}\left(\frac{d_{\text{rail}}'}{d_0}\right), \tag{12}$$

where

(i) the frequency band of interest for subway-induced vibrations is 1 Hz~80 Hz;

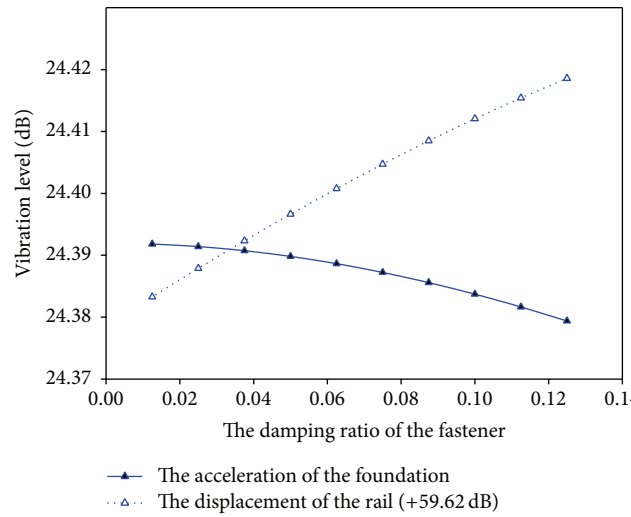

Figure 6: The displacement of the rail and the acceleration of the foundation with ξ_f when $k_f = 5 \times 10^7$ N/m, $\xi_{\text{ss}} = 0.125$, and $k_{\text{ss}} = 5 \times 10^6$ N/m.

(ii) $d_{\text{rail}}' = \sqrt{\sum_{f=1}^{80} |V_{\text{rail}}^{1(2)}(f)/(j\omega)|^2/80}$, $d_0 = 1 \times 10^{-12}$ m;

(iii) $a_f' = \sqrt{\sum_{f=1}^{80} |j\omega \cdot V_f^1(f) + j\omega \cdot V_f^2(f)|^2/80}$, $a_0 = 1 \times 10^{-6}$ m/s^2.

4. Optimization Variable Decision

According to the description of Sections 2 and 3, the vibration displacement of the rail and the vibration acceleration of the foundation will be influenced by the physical properties of the fasteners and the steel-springs, that is, the damping ratio of the fastener ξ_f, the stiffness of the fastener k_f, the damping ratio of the steel-spring ξ_{ss}, and the stiffness of the steel-spring k_{ss}. In order to decide which ones should be set as optimization variables, all physical parameters were analyzed firstly.

Considering the application of the fastener and the steel-spring in practice, vibration parameters of the floating slab track are supposed to be

(i) $0.025 \le \xi_f \le 0.25$;

(ii) 1×10^7 N/m $\le k_f \le 10 \times 10^7$ N/m;

(iii) $0.025 \le \xi_{\text{ss}} \le 0.25$;

(iv) 1×10^6 N/m $\le k_{\text{ss}} \le 10 \times 10^6$ N/m.

The calculation codes were built by the commercial software MATLAB. Figures 6–9 show the calculation results.

From Figures 7 and 8, the variation tendency of the displacement of the rail and the acceleration of the foundation is the same for the stiffness of the fastener and the damping ratio of the steel-spring. In other words, the displacement of the rail and the acceleration of the foundation will decrease with the increase of the stiffness of the fastener or the damping ratio of the steel-spring. So if we want to get the minimum displacement of the rail and the minimum acceleration of

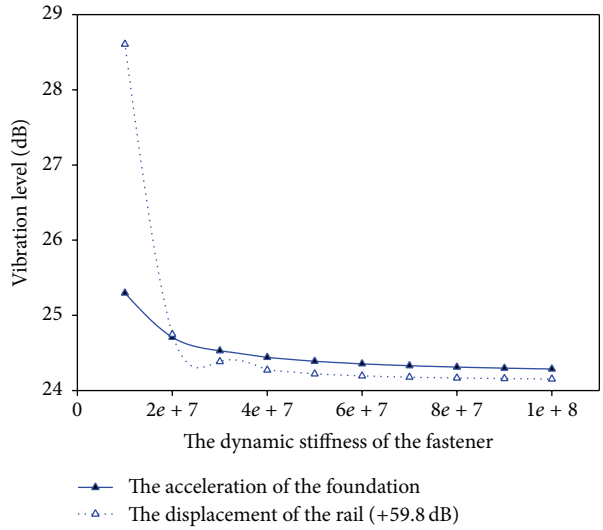

Figure 7: The displacement of the rail and the acceleration of the foundation with k_f when $\xi_f = 0.125$, $\xi_{ss} = 0.125$, and $k_{ss} = 5 \times 10^6$ N/m.

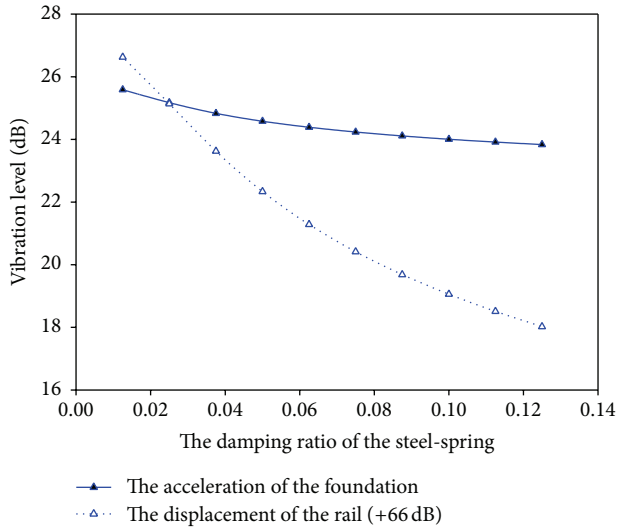

Figure 8: The displacement of the rail and the acceleration of the foundation with ξ_{ss} when $\xi_f = 0.125$, $k_f = 5 \times 10^7$ N/m, and $k_{ss} = 5 \times 10^6$ N/m.

the foundation, we only need to make the stiffness of the fastener and the damping ratio of the steel-spring maximum. Figure 6 shows that the vibration acceleration of the foundation will decrease and the rail displacement will increase with the increase of the damping ratio of the fastener. Figure 9 has the opposite regulation compared with Figure 6. In a word, the variation tendency of the objectives (the displacement of the rail and the acceleration of the foundation) is in conflict with the increase of the damping ratio of the fastener or the stiffness of the steel-spring.

Therefore, the damping ratio of the fastener and the stiffness of the steel-spring are set as optimization variables.

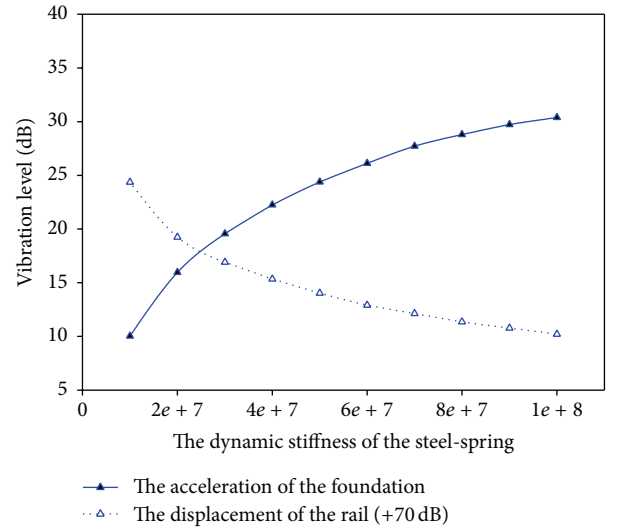

Figure 9: The displacement of the rail and the acceleration of the foundation with k_{ss} when $\xi_f = 0.125$, $k_f = 5 \times 10^7$ N/m, and $\xi_{ss} = 0.125$.

5. Multiobjective ACO

With the development of computer technology, swarm intelligence optimization algorithms, that is, Ant Colony Optimization (ACO), Particle Swarm Optimization (PSO), and so on, have attracted more and more attention. ACO is one of the most successful swarm intelligence optimization algorithms. It was proposed by Colorni et al. [12] to solve the Traveling Salesman Problem (TSP) in 1991, named ant system (AS), which takes inspiration from the foraging behaviors of the Argentine ants. In recent years, ACO has solved many combinatorial optimization problems of single-objective successfully [13, 14] and is being extended to obtain the solutions of the continuous problems [15] and multiobjective problems [16, 17].

In this section, multiobjective FHACO was employed [18]. The core thought of FHACO supposes that every ant deposits two kinds of pheromones, that is, the food pheromone and the nest pheromone. For this, the process of the foraging-homing for ant colonies is described as follows.

Each artificial ant randomly starts from the nest to the food source, following the food pheromone and depositing the nest pheromone on the path. Then, they come back, smelling the nest pheromone and laying the food pheromone on the ground.

5.1. Constructing the Initial Pareto Optimal Solution Set. According to the number of the design variables, the corresponding number of ant colonies was set. Take two design variables as an example.

If the designing variables are x_1 and x_2, $a_1 \le x_1 \le b_1$, $a_2 \le x_2 \le b_2$, two groups of ants will be set. And each group has Num ants, which are distributed to the designing space of the corresponding variable uniformly.

Therefore, every ant of the first group has a value

$$x_{1(i)} = a_1 + (i-1) \times \frac{(b_1 - a_1)}{(\text{Num} - 1)}, \tag{13}$$

in which $i = 1, 2, \ldots, \text{Num}$.

Similarly, each ant of the second group has a value given as

$$x_{2(j)} = a_2 + (j-1) \times \frac{(b_2 - a_2)}{(\text{Num} - 1)}, \tag{14}$$

where $j = 1, 2, \ldots, \text{Num}$.

An information exchange mechanism between two groups of the ants was built up. Then, Num^2 pairs of values of design variables $(x_{1(i)}, x_{2(j)})$ are formed, $i = 1, 2, \ldots, \text{Num}$, $j = 1, 2, \ldots, \text{Num}$.

Substituting $(x_{1(i)}, x_{2(j)})$ to the objective functions, the results of the multiobjective functions are obtained, that is, $f_1(x_{1(i)}, x_{2(j)})$ and $f_2(x_{1(i)}, x_{2(j)})$, $i = 1, 2, \ldots, \text{Num}$, $j = 1, 2, \ldots, \text{Num}$. According to the constraint conditions, nonfeasible solutions are excluded. Finally, the initial Pareto optimal solution set is built by comparison of the domination relations of the feasible solutions.

5.2. Updating the Initial Food Pheromone. Given that the initial food pheromone τ_{food} is the same, it cannot guide ants to find the optimal path. Consequently, we will update the initial food pheromone with the initial optimal paths obtained by the initial Pareto optimal solution set as shown below:

$$\tau_{\text{food}} \longleftarrow \tau_{\text{food}} + Q_c, \tag{15}$$

where $\tau_{\text{food}} = 0.01$ is the initial food pheromone of the initial optimal paths and Q_c is the tuning factor. Here, we let $Q_c = 0.5$.

5.3. The Foraging Process. Suppose that $f(x)$ is the original objective function and x is the original design variable whose minimum value is a and the maximum value is b. Let $f(x)$ be $f(x')$ by simple mathematical transform, in which $x' = (x - a)/(b - a)$, $x' \in [0, 1]$. Thus, the process of $f(x)$ optimization is the transformed process of $f(x')$ optimization.

Considering the searching space of x', the function $f(x')$ optimization process is simplified as an artificial ant makes a selection of ten decimal numbers whenever it takes a step except the first floor and the last floor (see Figure 8). When $|x' - 1| \leq \varepsilon$, we let x' be equal to 1, in which ε is a minimum value (1×1^{-d}). According to the complexity of the optimization problem, the number of floors is set as d.

Each artificial ant goes from the first floor (the nest) toward the last floor (the feeding source). $T(j, k-1)$ is the decimal number when the ant j is at the floor $(k-1)$. The ant j selects the decimal number of the next floor according to

$$T(j,k) = \begin{cases} \max\left\{\tau^k_{\text{food}-(T(j,k-1),T(j,k))}\right\}, & q < Q_0 \\ \text{randperm}, & q \geq Q_0, \end{cases} \tag{16}$$

in which q is a real random variable uniformly distributed in the internal $[0, 1]$, Q_0 is a tunable parameter controlling the influence of the pheromone, randperm is a number selected randomly from $(0, 1, \ldots, 9)$, and $\tau^k_{\text{food}-(T(j,k-1),T(j,k))}$ is the intensity of the food pheromone laid on the path between the number $T(j, k-1)$ and the number $T(j, k)$.

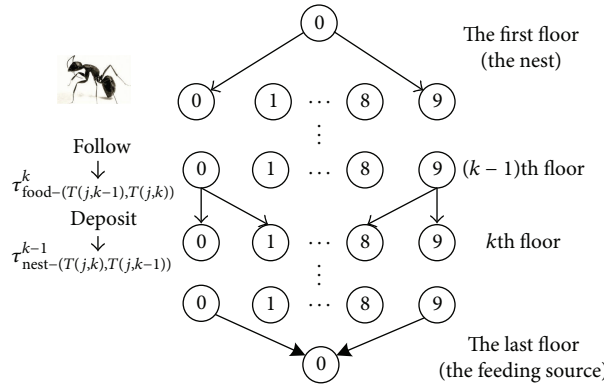

Figure 10: The foraging process to search the optimal results by ants.

When an ant finishes one step, that is, an ant arrives at the floor k from the floor $(k-1)$, the strength of the nest pheromone $\tau^{k-1}_{\text{nest}-(T(j,k),T(j,k-1))}$ laid on the path between the number $T(j, k)$ and the number $T(j, k-1)$ by the ant j should be updated as follows:

$$\tau^{k-1}_{\text{nest}-(T(j,k),T(j,k-1))} \longleftarrow (1 - \rho_{\text{nest}}) \times \tau^{k-1}_{\text{nest}-(T(j,k),T(j,k-1))} + \alpha, \tag{17}$$

where α is the modified coefficient of the intensity of the nest pheromone and ρ_{nest} is the local evaporation factor of the nest pheromone (see Figure 10).

5.4. The Homing Process. After all artificial ants arrive at the food source, each ant comes back smelling the nest pheromone laid in the foraging process. The method to select the decimal number of the $(k-1)$th floor when the ant j reaches at the floor k is described as follows:

$$T(j, k-1) = \begin{cases} \max\left\{\tau^{k-1}_{\text{nest}-(T(j,k),T(j,k-1))}\right\}, & q < Q_0 \\ \text{randperm}, & q \geq Q_0. \end{cases} \tag{18}$$

When the ant j arrives at the position $T(j, k-1)$ of the floor $(k-1)$, the intensity of the food pheromone $\tau^k_{\text{food}-(T(j,k),T(j,k-1))}$ laid on the path between the number $T(j, k)$ and the number $T(j, k-1)$ also should be updated:

$$\tau^k_{\text{food}-(T(j,k),T(j,k-1))} \longleftarrow (1 - \rho_{\text{food}}) \times \tau^k_{\text{food}-(T(j,k),T(j,k-1))} + \beta, \tag{19}$$

in which β is a constant to modify the intensity of the food pheromone locally and ρ_{food} is the local evaporation factor of the food pheromone.

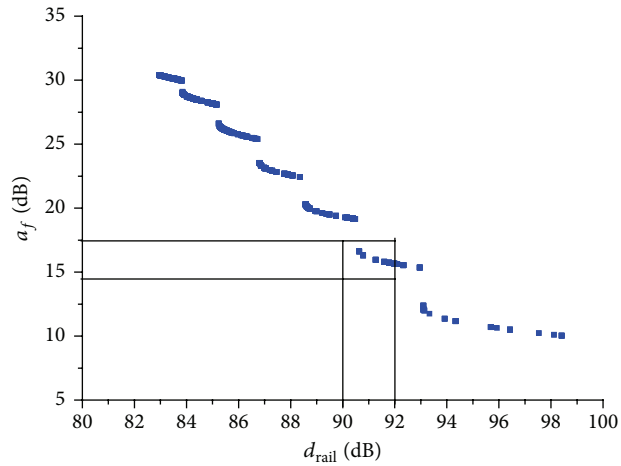

Figure 11: The Pareto optimal frontier of biobjective optimization.

5.5. Updating the Pareto Optimal Solution Set. After one iteration, every ant gets its own solution of the multiobjective optimization problem. In accordance with the constraint functions and the domination relations, we can make the Pareto optimal solutions and the Pareto optimal frontier be updated.

6. Biobjective Optimization

The parameters of the multiobjective ACO are set as follows: the floors d are 3, the ant population n is 20, the iteration number is 20, Q_0 is 0.3, the local evaporation factor of the nest pheromone ρ_{nest} is 0.5, the modified coefficient of the nest pheromone α is 0.5, the local evaporation factor of the food pheromone ρ_{food} is 0.5, and the modified coefficient of the food pheromone β is 0.5.

Using the program of the mathematical model of the steel-spring floating slab track coupled with the multiobjective ACO, we can obtain the Pareto optimal frontier (see Figure 11) and the Pareto optimal solution set for the problem proposed in Section 4. In many engineering problems, the designers only need to know the best optimum (lying on the Pareto optimal frontier) in the preferred zone [19]. In other words, we can get the correspondent designing variables from Figure 11 for the best objective values for the request of the engineering.

For example, if the planed d_{rail} and a_f are located in the black box, consequently, we can obtain the corresponding values of the damping ratio of the fastener and the stiffness of the steel-spring.

7. Conclusions

In conclusion, we modeled the floating slab track resting on the steel-springs by the four-pole parameter method. With this method, the influence of four vibration parameters, that is, the damping ratio of the fastener, the stiffness of the fastener, the damping ratio of the steel-spring, and the stiffness of the steel-spring, for the displacement of the rail and the acceleration of the foundation was researched. Results show that the variation tendency of the displacement of the rail and the acceleration of the foundation is the same for the stiffness of the fastener and the damping ratio of the steel-spring. However, they have the opposite variation tendency for the damping ratio of the fastener and the stiffness of the steel-spring.

In order to optimize the rail displacement and the foundation acceleration affected by the fastener damping ratio and the steel-spring stiffness at the same time, a multiobjective ACO was employed. Eventually, Pareto optimal frontier of the rail displacement and the foundation acceleration was derived. Furthermore, the desirable values of the fastener damping ratio and the steel-spring stiffness can be obtained according to the corresponding Pareto optimal solution set.

Conflict of Interests

The authors declare that there is no conflict of interests regarding the publication of this paper.

Acknowledgment

This project was supported by National Natural Science Foundation of China 51478353.

References

[1] W. Zhai, P. Xu, and K. Wei, "Analysis of vibration reduction characteristics and applicability of steel-spring floating-slab track," *Journal of Modern Transportation*, vol. 19, no. 4, pp. 215–222, 2011.

[2] K. Wei, S. Zhou, W. Zhai, J. Xiao, and M. Zhou, "The influencing factors of natural frequency optimization for steel-spring floating slab track in the metro-building integrated structure," *China Railway Science*, vol. 32, no. 4, pp. 8–13, 2011.

[3] K. Wei, S. Zhou, W. Zhai, J. Xiao, and M. Zhou, "Applicability of steel-spring floating-slab tracks of different natural frequencies for integrated metro-and-building structures," *Tumu Gongcheng Xuebao/China Civil Engineering Journal*, vol. 44, no. 11, pp. 134–142, 2011.

[4] D.-Y. Ding, W.-N. Liu, B.-C. Zhang, and X.-J. Sun, "Modal analysis on the floating slab track," *Journal of the China Railway Society*, vol. 30, no. 3, pp. 61–64, 2008.

[5] D. Ding, W. Liu, K. Li, and X. Sun, "Parametric study of the steel spring floating slab track," *China Railway Science*, vol. 32, no. 1, pp. 30–47, 2011.

[6] X. Lei and C. Jiang, "Analysis of vibration reduction effect of steel spring floating slab track with finite elements," *Journal of Vibration and Control*, 2014.

[7] A. Gu and H. Zhang, "Analyses of vibration isolation effect in different frequency band for steel-spring floating slab track," *Noise and Vibration Control*, vol. 29, no. 1, pp. 39–42, 2009.

[8] W. Liu, D. Ding, K. Li, and H. Zhang, "Experimental study of the low-frequency vibration characteristics of steel spring floating slab track," *Tumu Gongcheng Xuebao/China Civil Engineering Journal*, vol. 44, no. 8, pp. 118–125, 2011.

[9] K. Li, W. Liu, X. Sun, D. Ding, and Y. Yuan, "In-site test of vibration attenuation of underground line of Beijing metro line 5," *Journal of the China Railway Society*, vol. 33, no. 4, pp. 112–118, 2011.

[10] H. Jin and W.-N. Liu, "Vibration reduction optimization of ladder track based on an ant colony algorithm," *Journal of Central South University (Science and Technology)*, vol. 43, no. 7, pp. 2751–2756, 2012.

[11] Z. Cao, *Vibration Theory of Plates and Shells*, China Railway Publishing House, Beijing, China, 1983.

[12] A. Colorni, M. Dorigo, and V. Maniezzo, "Distributed optimization by ant colonies," in *Proceedings of the 1st European Conference on Artificial Life (ECAL '91)*, Paris, France, December 1991.

[13] C. Blum, "Ant colony optimization: introduction and recent trends," *Physics of Life Reviews*, vol. 2, no. 4, pp. 353–373, 2005.

[14] B. Chandra Mohan and R. Baskaran, "A survey: ant colony optimization based recent research and implementation on several engineering domain," *Expert Systems with Applications*, vol. 39, no. 4, pp. 4618–4627, 2012.

[15] F. A. C. Viana, G. I. Kotinda, D. A. Rade, and V. Steffen Jr., "Tuning dynamic vibration absorbers by using ant colony optimization," *Computers & Structures*, vol. 86, no. 13-14, pp. 1539–1549, 2008.

[16] M. Chica, O. Cordón, S. Damas, and J. Bautista, "Including different kinds of preferences in a multi-objective ant algorithm for time and space assembly line balancing on different Nissan scenarios," *Expert Systems with Applications*, vol. 38, no. 1, pp. 709–720, 2011.

[17] B. Yagmahan, "Mixed-model assembly line balancing using a multi-objective ant colony optimization approach," *Expert Systems with Applications*, vol. 38, no. 10, pp. 12453–12461, 2011.

[18] H. Jin and W. Liu, "Multi-objective function optimization based on ant colony algorithm with foraging-homing mechanism," *Application Research of Computers*, vol. 29, no. 11, pp. 4038–4040, 2012.

[19] S. K. Chaharsooghi and A. H. Meimand Kermani, "An effective ant colony optimization algorithm (ACO) for multi-objective resource allocation problem (MORAP)," *Applied Mathematics and Computation*, vol. 200, no. 1, pp. 167–177, 2008.